Optical Performance Monitoring in Reconfigurable WDM Optical Networks Using Subcarrier Multiplexing

Giammarco Rossi, Timothy E. Dimmick, and Daniel J. Blumenthal, *Senior Member, IEEE, Member, OSA*

***Abstract*—Optical performance monitoring (OPM) is an important approach to determine the quality of optical channels within an optical core network without passing data through optoelectronic regeneration at the monitor points. Using this approach, the quality or "health" of signals can be determined at arbitrary points in a network without knowledge of the transport history of the data or the details of the transmission path. We report experimental results on the use of subcarrier multiplexing (SCM) to perform a variety of monitoring functions including chromatic dispersion monitoring, wavelength registration, power monitoring, and signal-to-noise ratio (SNR) monitoring.**

***Index Terms*—Chromatic dispersion, optical networks, optical performance monitoring, power monitoring, signal-to-noise ratio monitoring, transmission performance, wavelength division multiplexing (WDM), wavelength registration.**

I. Introduction

THE DRIVE for high-bandwidth transparent wavelength division multiplexing (WDM) optical networks has spurred a need to develop new techniques to monitor channel performance and degradation without requiring optoelectronic-optic (OEO) conversion in the data path. Current optical network performance monitoring relies on SONET line terminating elements (LTEs) to determine the bit error rate (BER) and Q-factor from bits interleaved within the SONET frame or simple loss of signal (LOS) using power monitoring fiber taps. Causes of signal-to-noise (SNR) degradation and distortion are calculated by measuring the characteristics of active and passive optical network elements (e.g., optical amplifier noise figure, fiber dispersion) in advance. However, next generation optical networks will be dynamic (e.g., dynamic wavelength routing) and signals will traverse different complex paths consisting of fibers, amplifiers, optical add/drop multiplexers, optical crossconnects, etc. At any point within the network, each wavelength channel will have a different transport history including path and network elements that were traversed. As wavelengths are dynamically added to and dropped from the network, and switched between different fibers, the transport history will dynamically change. These dynamic changes will also drive the need for adaptive compensation techniques for gain equalization, chromatic dispersion compensation and polarization mode dispersion (PMD) compensation. Performance monitors that provide feedback for closed loop control of compensation elements will be critical. Additionally, component and fiber degradation and environmental changes will make it very difficult to manage these networks based on statically mapped network element and fiber properties.

Optical performance monitoring (OPM) is an approach that allows measurement of channel health and degradation without knowledge of the origin or transport history of the data. Direct measurements of, for example, BER are difficult as data patterns are not truly random and only a small percentage of optical power can be monitored without degrading the through-going signal. Yet sufficient power must be available for the monitor to be able to perform as well as the end point receiver in determining the BER. An alternative approach is to monitor various qualities of the data (e.g., chromatic dispersion, polarization mode dispersion, crosstalk, jitter, extinction ratio, channel power, SNR) indicative of channel degradation. It may also be desirable to characterize parameters of a data channel for corrective measures (such as dispersion compensation) or for network management purposes such as downgrading a channels bit rate or reporting degradation to the network management system (NMS) for alarm correlation and fault location.

In the OPM approach, the monitoring technique needs to operate on a signal that has traversed the optical path with the data whose health is to be determined. Subcarrier multiplexed (SCM) signals are a promising candidate to fulfill this requirement as they can be placed close to each optical carrier and either in-band or out of band electrically. Using SCM techniques, the signal can be monitored without the need to detect baseband data directly yet maintaining a strong correlation with the transport degradation mechanisms. Moreover, SCM can be used to carry control information in a circuit switched network or label information in packet-based architectures [1]–[3].

Other techniques to measure and control information in a WDM optical network have been studied and implemented

Manuscript received April 3, 2000; revised October 17, 2000. This work was supported by grants from Nortel Networks and a University of California Core Grant.

G. Rossi was with the Optical Communications and Photonic Networks Laboratory, Department of Electrical and Computer Engineering, University of California, Santa Barbara, CA 93106 USA. He is now with Agilent Technologies, Turin Technology Center, 10148 Torino, Italy.

T. E. Dimmick was with the Optical Communications and Photonic Networks Laboratory, Department of Electrical and Computer Engineering, University of California, Santa Barbara, CA 93106 USA, while on a leave of absence from the Laboratory for Physical Sciences, College Park, MD 20740 USA.

D. J. Blumenthal is with the Optical Communications and Photonic Networks Laboratory, Department of Electrical and Computer Engineering, University of California, Santa Barbara, CA 93106 USA.

Publisher Item Identifier S 0733-8724(00)11612-3.

including in-band signaling [4] and out-of-band signaling on a separate control wavelength. In comparison with transmitting information on a separate wavelength, the subcarrier per wavelength approach supports distributed network control with a synchronous recovery of wavelength identification, wavelength power, and control data, using a common circuit. The subcarrier portions of the transmitters and receivers can be fabricated using low cost monolithic-microwave integrated circuit (MMIC) technology that has been developed for wireless communications [2] or simple fiber-optic techniques. Potential limitations to OSCM include fiber nonlinearities and dispersion and detector saturation. However, crosstalk due to fiber four-wave mixing [5] is low as there is a single subcarrier per wavelength and the relative power of the subcarrier component is much less than the baseband component of the optical signal. Signal cancellation and fading due to dispersion can be overcome using suppressed carrier receivers as described in this paper and in [6] and single sideband subcarrier modulation techniques [7]. Monitoring of many subcarrier channels using a single photodetector can be achieved with new high-power traveling wave photodetector designs [8].

In this paper, we describe several techniques for monitoring key parameters of optical signals using SCM signals. Techniques for monitoring WDM channel power, optical SNR, and accumulated dispersion are presented. The intent of this paper is to describe a set of optical subcarrier-based measurements that can be used to determine the health of WDM baseband channels.

II. Optical Performance Monitoring

Future WDM optical networks will utilize dynamic wavelength routing to implement "lightpaths" [9], [10] through optical nodes using components like photonic crossconnects (PXCs), optical add/drop multiplexers (OADMs), optical amplifiers (OAs), adaptive gain equalizers (GEs), and dispersion compensation (DC) elements, as illustrated in Fig. 1(a). It is expected that switching these lightpaths optically will have a positive impact on cost, network utilization, and management in the networking layer [11] analogous to the impact on cost that erbium-doped fiber amplifiers (EDFAs) had on regeneration in transmission links.

An important issue in network management and survivability is the ability to measure the performance of optical data, detect degradation and failures, and provide means of failure location and isolation. The optical performance monitoring (OPM) approach deviates from traditional approaches in several ways. Presently, link parameters (e.g., dispersion, loss) are quantified on a link-by-link basis, typically under static conditions. The proposed OPM approach measures the condition of signals at various points within the network without detailed knowledge of the lightpath or the network elements and links that it traverses in a real-time dynamic environment. Only the resulting effects of SNR degradation and distortion are measure and utilized in determining the channel performance. This approach is illustrated in Fig. 1(a) where various OPM elements are used to measure relevant parameters for adaptive network elements and the overall health of DWDM signals.

Historically, the requirement to "recover" bits at every network element has dominated the network architecture. Traditional OEO regenerators [illustrated in Fig. 1(b)] have provided the means to analyze bits with various tradeoffs in the cost, complexity, scalability, and reliability of WDM regeneration points. The multichannel optical amplifier is an example of DWDM network elements that provides benefits that outweigh the need to look at bits. PXCs and OADMs will be used to groom wavelengths and fibers and have the potential to alleviate the need to OEO terminate every lightpath at each network element. The OPM approach more closely follows the configuration in Fig. 1(c) where a portion of the optical power is removed from the fiber and converted to an electronic signal for performance monitoring after possible optical signal processing. The problem that arises when trying to implement the approach in Fig. 1(c) results from the need to measure the performance with minimal disturbance to the signals in the fiber. The OE interface used at the tap must have a better sensitivity than a receiver used to recover the signal downstream. This is possible if the tap receiver is optically pre-amplified and the downstream losses and distortion are limited.

The channel BER is one of the most important parameters to measure and is in general the most difficult to measure directly for a signal at the output of a power tap. Qualities of the signal other than the BER that can be measured using OPM include:

- SNR and Q Factor monitoring
- Extinction Ratio Monitoring
- Loss and power monitoring
- Dispersion monitoring (Chromatic and PMD)
- Nonlinear distortion monitoring
- Channel equalization
- Crosstalk monitoring
- Wavelength registration
- Network state monitoring
- Clock monitoring in 2R regenerators
- Bit rate monitoring

Estimation of the BER from parameters like the Q-factor can be performed if the eye closure is due to Gaussian-like noise sources only [12]. The presence of non-Gaussian noise sources, crosstalk, and distortion mechanisms will lead to errors in estimating the BER using the Q-factor. It may be possible to utilize other SNR degradation and signal distortion factors to estimate the BER, as shown in Fig. 2. The latter is not a subject addressed in this paper.

The primary causes of degradation of the BER that can be monitored using OPM include:

Noise: Caused by random signal fluctuations that can be treated as a Gaussian process and can be signal level dependent. Examples include optical amplifier noise and laser noise.

Distortion: Caused by nonlinearities or fiber dispersion effects that may be signal level and pattern dependent and can lead to bursty errors and BER floors. Examples include laser, optical amplifier and fiber nonlinearities, laser diode

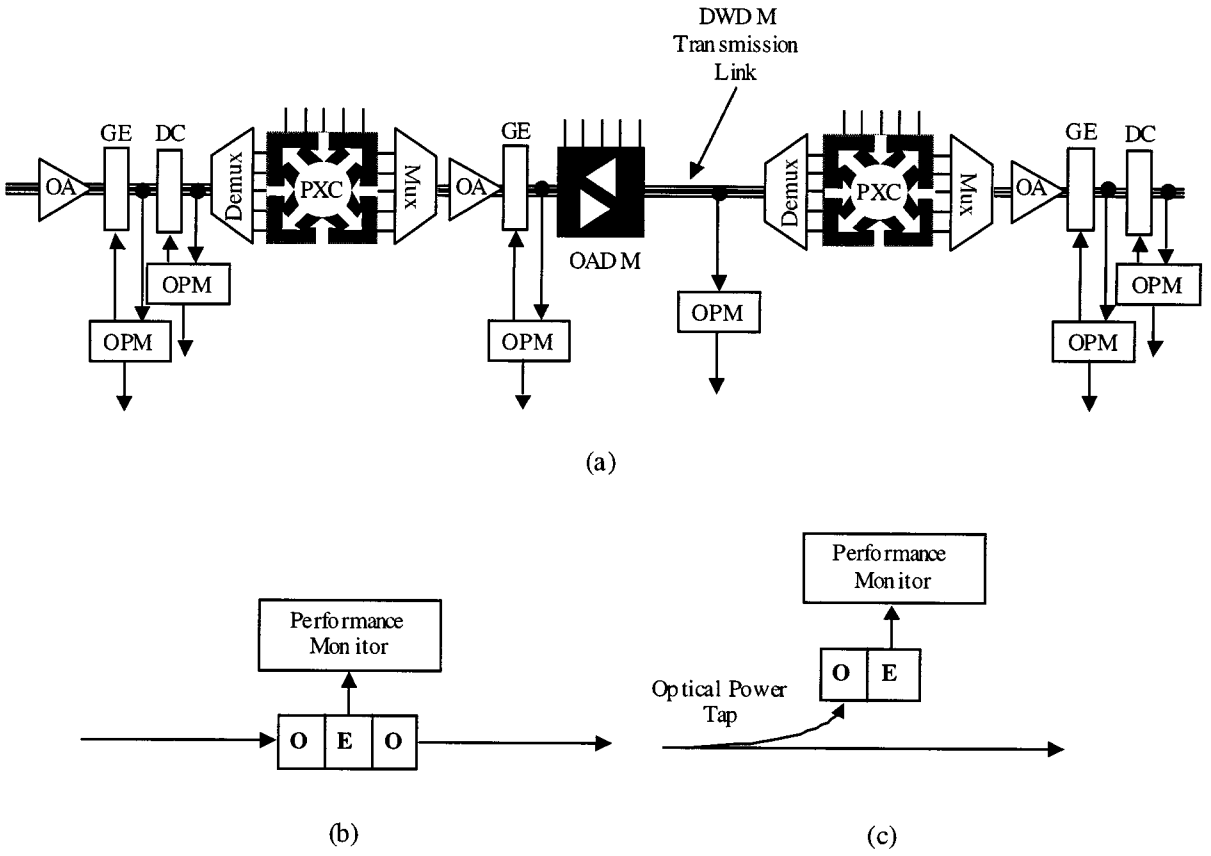

Fig. 1. (a) Illustration of a reconfigurable WDM optical network with various network elements and placement of OPM elements. Performance monitoring using (b) OEO regeneration and (c) optical power tap approaches.

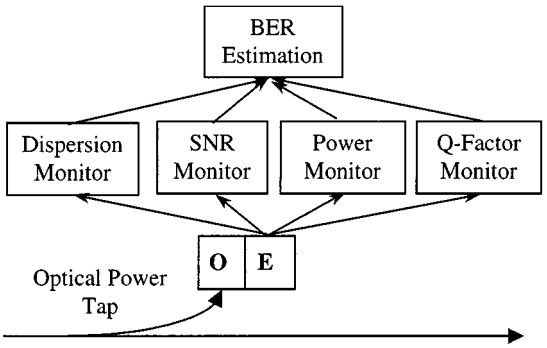

Fig. 2. Potential utilization of various OPM metrics to estimate the BER.

bit pattern dependent response, receiver bit pattern dependent response, chromatic and polarization mode dispersion, in-band crosstalk, out-of-band crosstalk, and phase induced intensity noise.

Crosstalk: It is important to mention that interferometric and nonlinear crosstalk are bit pattern effects that may or may not be treated as noise. This depends on the number of interfering terms and the nature of the interfering signals. Other issues that must be addressed with any performance monitoring technique include those listed below.

Power Detection: Techniques to identify loss of signal and changes in optical power for power equalization. Power detection must distinguish between channel loss and "strings of zeros" transmission.

Frequency Monitoring: Frequency selective elements and frequency agile sources must be within 1% of channel bandwidth. This standard must be applied to stabilization of frequency dependent components

III. Subcarrier Signals for Monitoring

In this paper we report several OPM techniques based on optical subcarrier multiplexing (OSCM). The strengths of this approach lie in the simplicity of using double sideband subcarrier signal transmission and the fact that these signals travel the complete optical path with the baseband signal to be measured. The subcarrier signals can be recovered using techniques described below that are immune to fiber dispersion induced fading. Since a unique subcarrier frequency can be allocated to each wavelength, a complete set of subcarrier multiplexed signals can be recovered from a WDM optical stream using a single photodetector. The use of subcarriers can be contrasted to other approaches using low frequency pilot tones for wavelength registration [13]. However, pilot tones limit the amount of information that can be carried on the monitor to several tens of kilohertz limits the number of tones that can be placed below a digital signal and the resolution with which certain parameters like dispersion can be measured.

IV. SCM Generation and Detection

Several methods have been published for the generation of hybrid baseband/SCM signals. These include combining baseband and subcarrier signals electronically followed by direct laser modulation [14] or combining these signals electrooptically with a differentially driven Mach–Zehnder integrated-optic modulator [15]. Using a single modulator to generate the baseband data and the subcarrier results in a power penalty that can be minimized provided the subcarrier amplitude is sufficiently small. In our experiments we measured a power penalty to the baseband data of between 0.5 and 2 dB depending on the amplitude of the subcarrier signal relative to the baseband signal. In the work described in this paper, the differentially driven modulator method was used. A schematic diagram of the hybrid baseband/SCM transmitter is shown in Fig. 3. In our transmitter, the baseband data and the SCM signal are encoded on the optical carrier by means of a dual-arm Mach–Zehnder $LiNbO_3$ electro optical modulator with a 3 dB bandwidth of 18 GHz. The baseband data was encoded on one arm of the modulator, while the other arm was driven with a 16.7 GHz RF tone. In some of the performance monitoring experiments, the subcarrier tone was also amplitude modulated to provide information beyond that available with the pure DSB subcarrier.

Demultiplexing and detection of the SCM signal may be accomplished at any point within the network by tapping a small portion of the transmitted signal. Detection of the SCM signal involves either electrical bandpass filtering after photodetection or optical pre-filtering prior to photodetection. For DSB subcarrier transmission, optical pre-filtering can be used for carrier suppression prior to detection in order to overcome signal fading caused by fiber dispersion [6].

V. Channel Identification and Power Monitor

The knowledge of which wavelengths are currently on a WDM link and their relative power are important parameters for optical networks. Optical amplifiers tend to favor some wavelength channels at the expense of others introducing power differences since small differences in power following one amplifier will be exaggerated as many amplifiers are often concatenated. Even carefully designed wavelength flattened links can have problems brought about by aging components.

An optical power monitor tap that uses high-frequency subcarriers [16] is depicted in Fig. 4. Shown in this figure is a tap capable of monitoring four wavelengths simultaneously. In this approach, each wavelength carries with it a unique DSB subcarrier frequency. This permits monitoring of all channel powers without the need for demultiplexing in the optical domain and separate detectors for each wavelength. Since the subcarrier power relative to the channel power is fixed at the transmitter, variations in the channel power due to wavelength dependent gain or loss can be immediately detected as variations in the subcarrier power. A power monitor of this type has been used within a feedback loop with an acousto-optic tunable filter to equalize the per wavelength power in a WDM experiment [17]. It is necessary that the ratio between optical signal power and RF power in the corresponding subcarrier signal be fixed within a specified tolerance for all transmitters in the network. This scheme can also be used for channel identification since it is possible to determine what wavelengths are present on a given link by simply detecting which subcarrier frequencies are present.

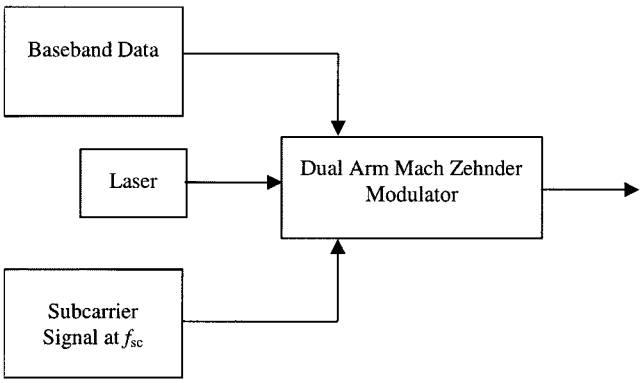

Fig. 3. Hybrid baseband data/SCM transmitter.

VI. Optical and Electrical Signal to Noise Ratio Monitor

Monitoring of SNR on a per-channel basis is needed to access the health of signals that have traversed optical amplifiers and loss elements. Different wavelengths follow different paths, through various elements with wavelength dependent gain or loss. As a consequence, the SNR may vary from channel to channel and from point to point in the network making monitoring and control of SNR key to all optical networking.

A common method of measuring SNR relies on optical spectrum analysis wherein the noise level is measured adjacent to the signal wavelength and the OSNR is calculated by interpolation [18], [19]. The accuracy of this technique is degraded by the presence of multiple filtering elements in the signal path. Spectral shaping caused by these elements leads to unbearable underestimation errors. Several other OSNR measurement techniques have recently been reported [20]–[23].

Subcarriers provide a reliable and simple means for monitoring the OSNR. The OSNR can be determined by measuring the electrical carrier-to-noise ratio (CNR) at the detector. The OSNR is given by

$$\mathrm{OSNR} = \sqrt{\frac{B_{ESA}}{\Delta\upsilon}}\,\frac{\mathrm{CNR}}{m^2} \tag{1}$$

where

- CNR carrier-to-noise ratio as measure with an electrical spectrum analyzer with resolution bandwidth B_{ESA};
- $\Delta\nu$ optical bandwidth;
- m modulation depth of the subcarrier.

Equation (1) is valid when the noise of the photodetector is negligible and the optical noise is dominated by the amplifier spontaneous-spontaneous beat noise. The resolution bandwidth of the spectrum analyzer may be reduced in order to improve the accuracy and increase the sensitivity of the monitor. This increases the measurement time.

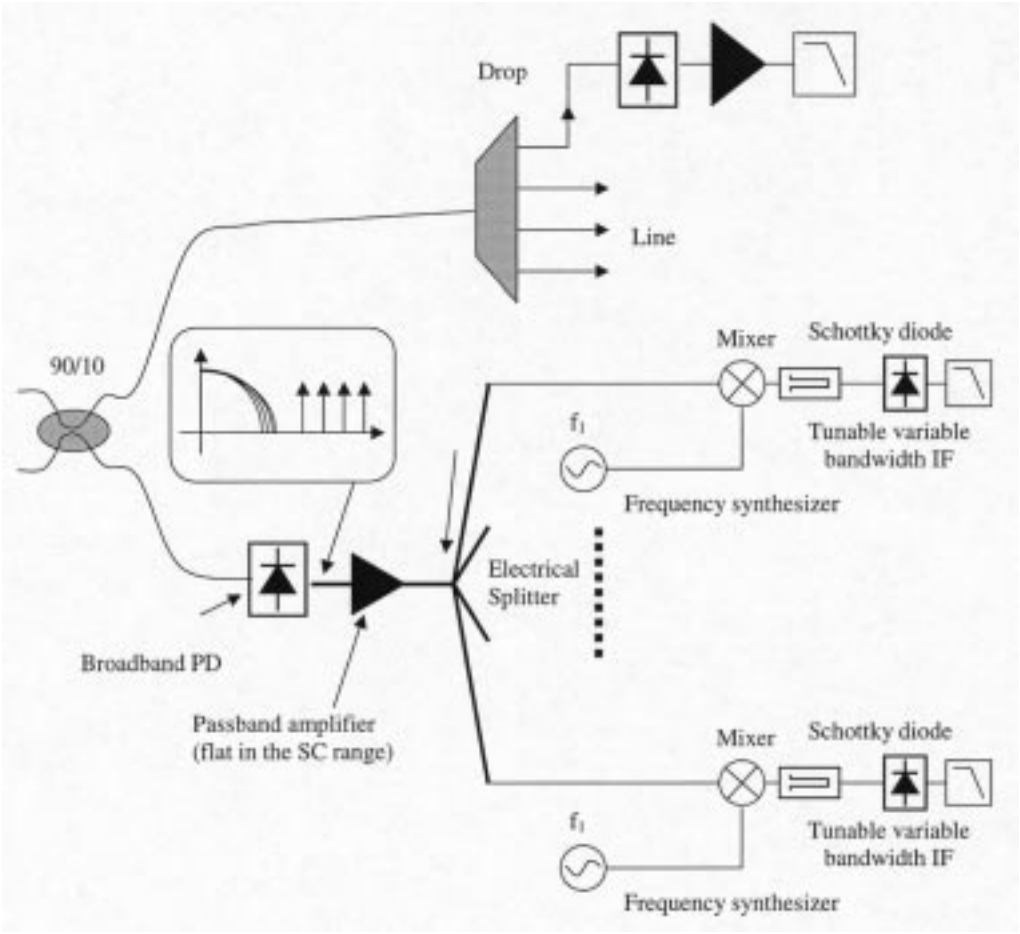

Fig. 4. Tap for power monitor.

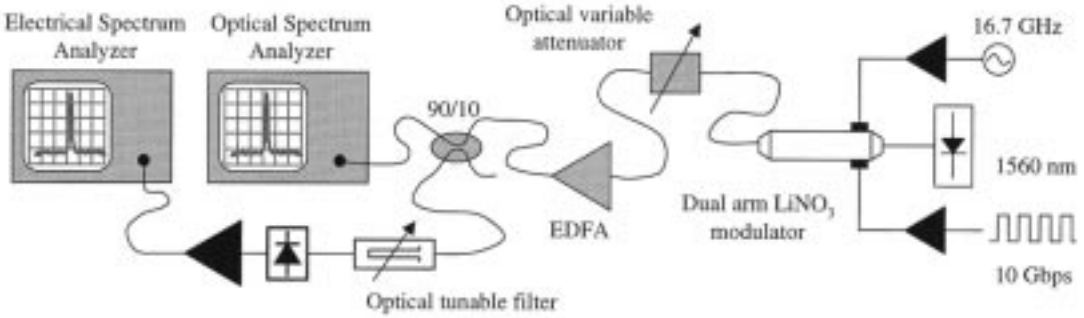

Fig. 5. Set-up for OSNR monitor.

When the input power is too low, the photodetector electrical noise is significant and has to be calibrated out. In this regime, (1) is still valid but with and effective CNR given by

$$\mathrm{CNR}_{\mathrm{eff}} = \left(\mathrm{CNR}^{-1} - \frac{N_{PD}B_{ESA}}{P_{\mathrm{SCM}}}\right)^{-1} \tag{2}$$

where N_{PD} is the photodetector noise power spectral density.

A. Experimental Results

The experimental set-up is shown in Fig. 5 and the transmitter architecture of Fig. 4 was used to generate the DSB subcarrier multiplexed signal. An optical variable attenuator is used to control the power injected into the EDFA to vary the output signal to noise ratio. A small part of the signal power is tapped out through a 90/10 coupler and a tunable filter ($\Delta\nu = 0.8$ nm) is used to select the proper channel. A broadband high-speed photodetector followed by a front-end amplifier is used for optoelectronic conversion. Finally, an electrical spectrum analyzer (ESA) is used to measure the CNR. The OSNR is also measured with a conventional optical spectrum analyzer.

The results of the measurement are reported in Fig. 6. This technique can predict the OSNR with less than 2 dB error over almost 25 dB range and less than 1 dB where the OSNR is less than 20 dB, a critical range. The measurement is accurate even

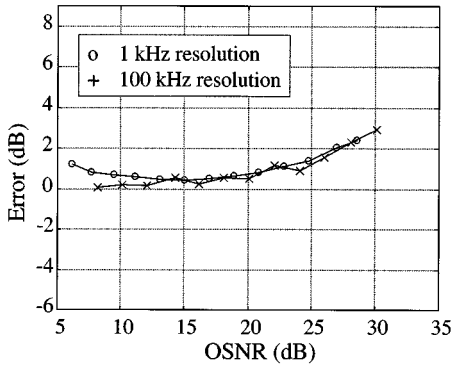

Fig. 6. Error between the OSNR measured with the OSA and the ESA (x marker for -30 minimum power dBm 100 kHz resolution bandwidth; o marker -40 dBm, 1 kHz).

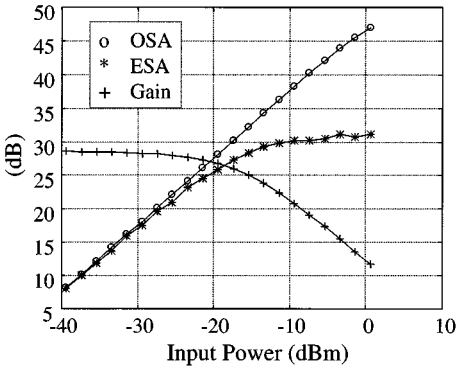

Fig. 7. OSNR measured with an optical (squares) and electrical (triangles) spectrum analyzer (left y scale) and EDFAs gain (right y-scale) in function of the EDFA input power.

when the input power to the photodetector is changed provided that the resolution bandwidth of the photodetector is properly adjusted. For OSNR higher than 30 dB, our method diverges from the optical technique since, as shown in Fig. 7, the amplifier starts to saturate and the hypothesis supporting (1) is not valid.

B. Chromatic Dispersion and PMD

It is well known that fiber chromatic dispersion induces fading in double sideband subcarrier signals, which can make this type of measurement impractical for link distances beyond several tens of kilometers. Possible solutions are to either transmit and detect single sideband subcarriers [7] or to use suppressed carrier optical receivers based on optical filters [24].

PMD causes a wavelength dependent variation of the polarization state. Therefore, at the receiver, the expression for single sideband subcarrier photocurrent will be

$$I_{\mathrm{SCM}}\,(\vec{p}_O \cdot \vec{p}_{\mathrm{SCM}})\, mI_O \cos(\omega_{\mathrm{SCM}} t + \varphi) \tag{3}$$

where

ω_{SCM} subcarrier angular frequency;

I_O optical carrier photocurrent;

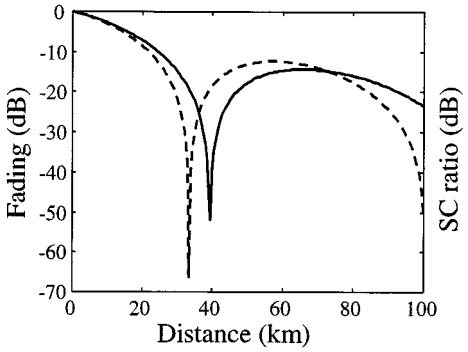

(a)

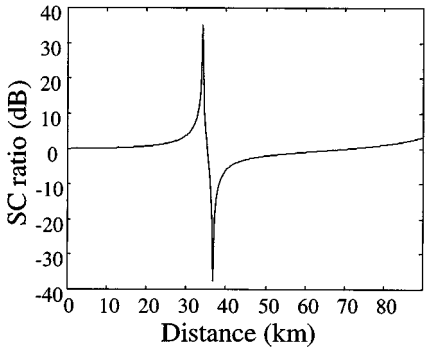

(b)

Fig. 8. Simulated results of subcarrier fading for (a) frequencies f_1 and f_2 and (b) the ratio f_1/f_2.

$\vec{p}_O \cdot \vec{p}_{\mathrm{SCM}}$ scalar product between the states of polarization of the optical carrier and of the subcarrier whose effect is to produce an effective modulation depth lower the actual one.

This results in an underestimation of the OSNR. An *a priori* knowledge of the modulation depth together with the measurement of I_O can be used to calibrate this error out.

VII. Chromatic Dispersion Monitor

In this section,we describe two methods for monitoring the accumulated dispersion affecting a data channel without recovering the baseband data. The first method is extremely simple to implement but is limited to the measurement of small amounts of accumulated dispersion. The second method involves a more complex tap monitor but is capable of more accurately measuring very large amounts of dispersion.

A. Subcarrier Ratio Method

In this technique, we take advantage of what is usually considered a liability of subcarrier multiplexing, namely, the fading of the subcarrier signal that occurs as a result of accumulated dispersion. As the subcarrier signal traverses a dispersive fiber link, the subcarrier sidebands experience a relative phase delay that increases with the accumulated dispersion. This phase delay reduces the received subcarrier power measured at the detector. If the sidebands accumulate a total phase delay of □ the subcarrier power measured at the detector goes to zero. In a simple fiber span of loss per unit length α, length L, and dispersion

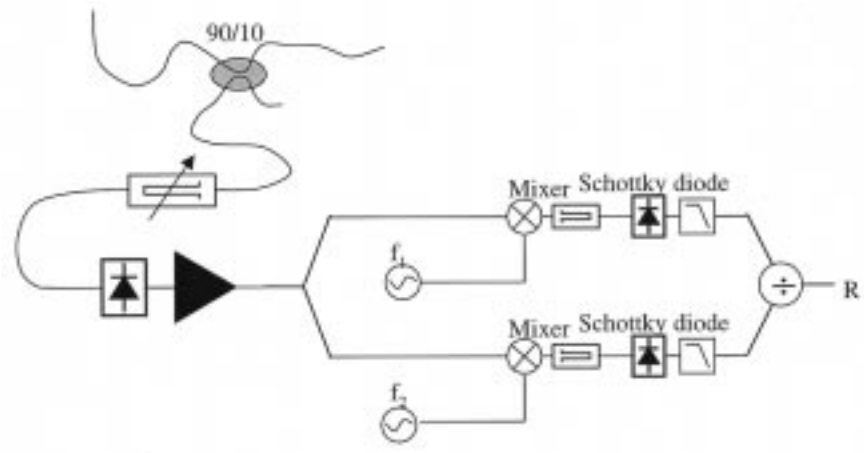

Fig. 9. Subcarrier ratio method dispersion monitor.

coefficient D, a subcarrier signal with initial power A, and frequency f will have a detected power

$$P = Ae^{-\alpha L}\cos^2\left(\frac{\pi DL\lambda^2 f^2}{c}\right) \tag{4}$$

where A is an unknown constant that accounts for the loss and gain elements that the signal experiences.

The received power will go to zero when

$$DL = \frac{C}{2\lambda^2 f^2}. \tag{5}$$

It is important to note that (4) and (5) are only valid when subcarrier signal is not chirped. Upon examination of (5) we see that higher frequency subcarrier signals fade faster (with less accumulated dispersion) than lower frequency signals. To illustrate this effect, (4) is plotted in Fig. 8(a) as a function of L for subcarrier frequencies of 9.6 GHz and 10.4 GHz. For the plot we let $\lambda = 1550$ nm, $D = 18$ ps/nm•km, and $\alpha_{\rm dB} = 0.2$ km^{-1}.

If we prepare a subcarrier signal at the transmitter composed of two subcarrier frequencies f_1 and f_2, then it is possible to measure the accumulated dispersion this signal (and the baseband data signal as well) has experienced by simply measuring the ratio of the electrical power at frequency f_1 to that at frequency f_2 received at the monitor point. This way we avoid the dependence of measured power upon the unknown factor A.

A dispersion monitor tap that implements this technique is shown in Fig. 9. The output of the dispersion monitor is given as

$$R = \cos^2\left(\frac{\pi DL\lambda^2 f_1^2}{c}\right) \Big/ \cos^2\left(\frac{\pi DL\lambda^2 f_2^2}{c}\right) f_1 < f_2. \tag{6}$$

Equation (6) is plotted in Fig. 8(b) as a function of L with $\lambda = 1550$ nm, $D = 18$ ps/nm•km, $f_1 = 9.6$ GHz, and $f_2 = 10.4$ GHz. Equation (6) uniquely determines the accumulated dispersion up to a maximum DL product of $c/2\lambda^2 f_2^2$.

B. Optical Side-Band Suppression Method

In this technique, a DSB subcarrier signal is combined with the baseband data at the transmitter, as illustrated in Fig. 1. The subcarrier tone is amplitude modulated by a low frequency signal. The transmitter architecture is the same as was described in [15] where it was used to encode labels on data packets. The spectrum of the transmitter output (depicted in the inset of Fig. 3) shows the double sideband nature of the subcarrier signal. When this signal is propagated through dispersive fiber, the dispersion induces a relative time delay between the subcarrier sidebands given by [25]

$$\Delta t = f_{SC}\frac{\lambda^2}{c} DL. \tag{7}$$

By measuring the relative phase delay between the sidebands, it is possible to determine the amount of dispersion (DL product) the baseband signal has experienced.

It is clear from (7) that by choosing a subcarrier frequency that is large compared to the bit rate of the underlying data, very sensitive measurement of accumulated dispersion is possible. Unfortunately, measurement of the subcarrier phase delay alone limits the maximum dispersion that can be measured to the period of the subcarrier signal. It is possible to overcome this limit to measurement of high values of dispersion by measuring the delay experienced by the relatively low frequency modulation applied to the subcarrier signal. In this case the time delay between the modulation on the upper and lower sidebands is given by [25]

$$\Delta t = 2f_{SC}\frac{\lambda^2}{c} DL. \tag{8}$$

In this way, the range of the measurement is extended to delays comparable with the period of the modulation applied to the subcarrier signal, much longer than in the previous case.

The tap architecture we developed for monitoring accumulated dispersion combines these two techniques to make possible the measurement of a wide range of dispersion with high resolution. A schematic diagram of the tap architecture is shown in Fig. 10. Referring to the figure, a portion of the optical signal is removed from the trunk fiber, divided into two and transmitted through optical filters that suppress the upper and lower sidebands, respectively. Following the filtering, both signals are detected and the baseband data is removed using electrical band-

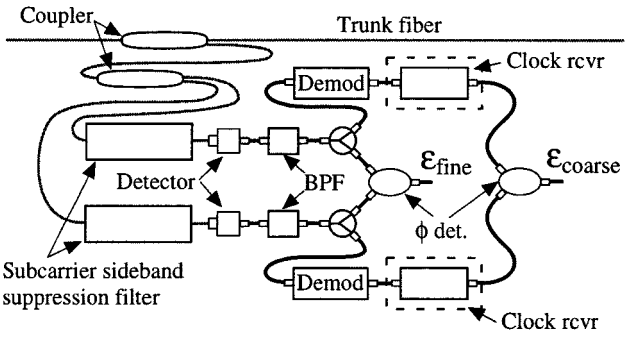

Fig. 10. Optical sideband suppression dispersion monitor. $BPF =$ electrical bandpass filters. $\varepsilon_{\rm coarse}$ and $\varepsilon_{\rm fine}$ are outputs indicating the dispersion affecting the optical signal.

pass filters. Each of these signals is then further divided with one output providing an input to a phase detector and the other output being directed to an amplitude demodulator. The phase detector produces a signal proportional to the phase difference between the subcarrier signals. This provides a fine measurement of dispersion as explained earlier, according to (7). The outputs of the amplitude demodulators are directed to a second phase detector that provides a coarse measurement of dispersion. The coarse measurement may be used to resolve phase ambiguities in the fine measurement. A clock recovery step is only necessary when data is encoded on the subcarrier. In that case the recovered clock is input to the second phase detector to obtain the coarse measurement.

1) Experiment and Simulation: A proof of principle experiment was conducted to validate this approach. The transmitter in the experiment made us of an 18 GHz $LiNbO_3$ Mach–Zehnder modulator to simultaneously encode baseband 2.5 Gb/s data and a 16.4 GHz subcarrier on a 1560-nm wavelength DFB laser. The subcarrier was amplitude modulated with a dc offset, 410-MHz sinusoidal tone.

The optical signal was propagated through varying lengths of step index, single mode fiber to simulate different DL products. At the end of the link the signal was optically amplified and split into two. On one arm the baseband data were detected, while the other was input to the dispersion monitor. The dispersion monitor followed the design illustrated in Fig. 10 with the exception that following the electrical bandpass filters the signals were amplified and input to a sampling oscilloscope. The waveforms were acquired with the oscilloscope and transferred to a computer where the phase detection and demodulation functions were performed in software. The most critical elements in the dispersion monitor are the optical filters that perform the sideband rejection. In our experiment these were tunable bandpass filters (FWHM equal to 0.2 nm) adjusted to provide maximum rejection of the unwanted sideband while producing minimum attenuation of the desired sideband. Unfortunately, one of these filters did not perform as well as the other. The upper filter provided 24.3 dB of rejection but the lower filter provided only 14.8 dB of rejection.

Fig. 11 shows the results of the demonstration of the dispersion monitor. In Fig. 11(a), the coarse and fine delays are plotted as a function of fiber length. Also plotted in the figure (the solid line) is the theoretical curve given by (7). The coarse delay has been divided in two [(7) and (8) differ by a factor of two] so that both the coarse and the fine measurements can be compared to the same theoretical curve. The dashed lines are upper and lower bounds for the coarse measurement obtained by adding (subtracting) one half of the subcarrier period to (from) the theoret-

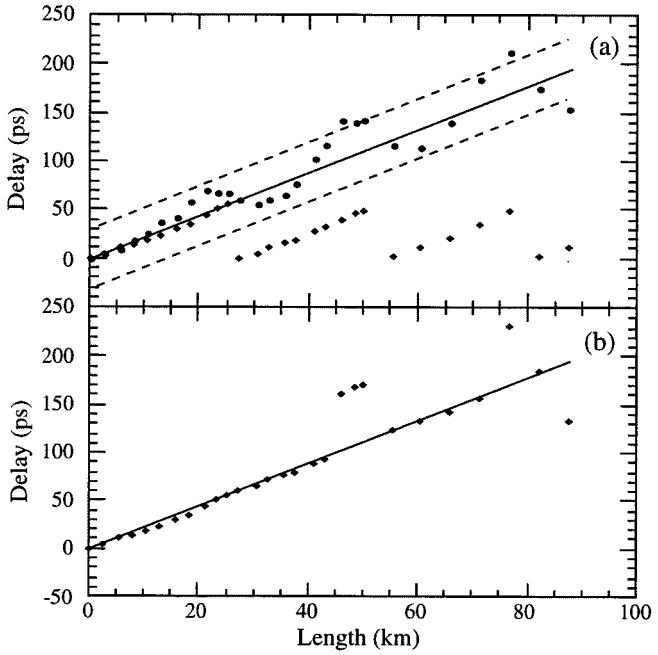

Fig. 11. Results of a proof of principle experiment. (a) Measured coarse delay divided by two (•) and fine delay (♦) plotted as a function of fiber length. The solid line is the theoretical delay given by (7). (b) The dashed lines are upper and lower bounds for the course measurements fine delay versus fiber length after it has been unwrapped and the ambiguities resolved.

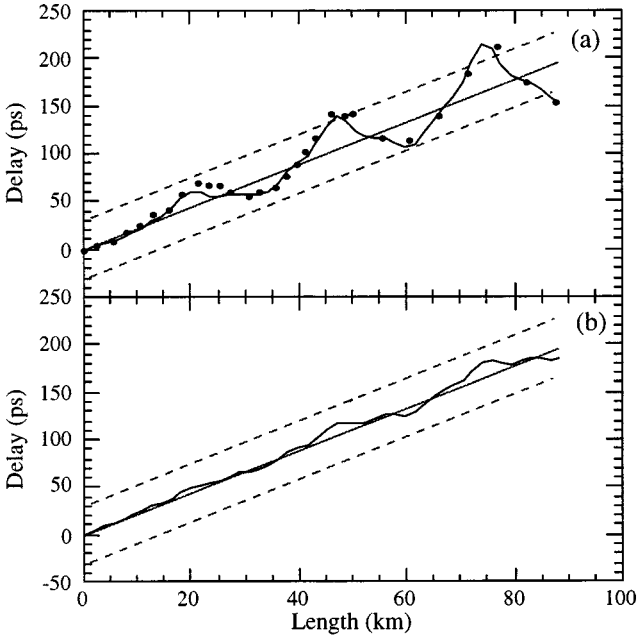

Fig. 12. Results of simulation and experiment. (a) Measured coarse delay (•) compared to the results of a simulation (solid line). (b) Simulation showing predicted coarse phase measurement with optical filters providing 30 dB of sideband rejection.

ical curve. Provided the coarse delay measurements fall within these bounds it is possible to correctly determine the proper order of the fine phase measurements. Fig. 11(b) shows the fine phase data after it has been unwrapped. Evident in the figure are some errors that resulted from coarse phase measurements that exceeded the limits shown in Fig. 11(a). We have determined through system simulation that these errors are a direct result of the poor sideband extinction obtained from the sideband rejection filter. Fig. 12(a) shows the results of our simulation where measured results are shown as points and the solid line is the output of the simulator. Excellent agreement between simulation and experiment is obtained. Fig. 12(b) shows the coarse delay as a function of length that would be obtained (according to our simulation) with filters that provide 30 dB of sideband suppression. Results from the simulator show that using the coarse measurement it is possible to resolve the ambiguities in the fine measurements to a time delay equal to the full period of the modulation applied to the subcarrier. This delay is equivalent to that produced by about 500 km of standard fiber or an equivalent DL product of 9167 ps/nm.

VIII. Conclusions

We have proposed and demonstrated the concept of optical performance monitoring using optical subcarriers where the health of WDM channels may be determined without prior knowledge of the data route and network elements that a lightpath traverses. This approach is critical to next generation WDM dynamically reconfigurable networks where the history of traffic at any point is unknown and the dependence on OEO regenerators is decreased. OPM techniques can be used to report degradation and failures to network management systems for fault isolation and network restoration. We have presented experimental results for a set of OPM functions including multichannel power monitoring, optical signal to noise ratio monitoring and chromatic dispersion monitoring. Results for OSNR monitoring with less than 2 dB error over 25 dB dynamic range were presented. Two techniques were presented for chromatic dispersion monitoring with capabilities to perform course and fine measurements over a dynamic range of 250 ps.

Acknowledgment

The authors would like to thank Dr. B.-E. Olsson and R. Doshi for their help in the laboratory aspects of this work.

References

[1] M. Cerisola, T. K. Fong, R. T. Hofmeister, L. G. Kazovsky, C. L. Lu, P. Poggiolini, and D. J. M. Sabido, "CORD—A WDM optical network: Control mechanism using subcarrier multiplexing and novel synchronization solutions," in *Proc. Int. Conf. Communications*, Seattle, WA, June 1995, pp. 261–265.

[2] D. J. Blumenthal, J. Laskar, R. Gaudino, S. Han, M. D. Shell, and M. D. Vaughn, "Fiber-optic links supporting baseband data and subcarrier-multiplexed control channels and the impact of MMIC photonic/microwave interfaces," *IEEE Trans. Microwave Theory Tech.*, vol. 45, pp. 1443–1452, Aug. 1997.

[3] D. J. Blumenthal, A. Carena, L. Rau, V. Curri, and S. Humphries, "All-optical label swapping with wavelength conversion for WDM-IP networks with subcarrier multiplexed addressing," *IEEE Photon. Technol. Lett.*, vol. 11, pp. 1497–1499, Nov. 1999.

[4] G. K. Chang, G. Ellinas, J. K. Gamelin, M. Z. Iqbal, and C. A. Brackett, "Multiwavelength reconfigurable WDM/ATM/SONET network testbed," *J. Lightwave Technol.*, vol. 14, pp. 1320–1340, June 1996.

[5] A. R. Chraplyvy, "Limitation on lightwave communications imposed by optical-fiber nonlinearities," *J. Lightwave Technol.*, vol. 8, pp. 1548–1557, Oct. 1990.

[6] G. Rossi, O. Jerphagnon, B. E. Olsson, and D. J. Blumenthal, "Optical SCM data extraction using a fiber loop mirror for WDM network systems," in *Tech. Dig, OFC'2000*, Baltimore, MD, USA, Mar. 2000, paper FD7, pp. 74–76.

[7] G. H. Smith and D. Novak, "Broad-band millimeter-wave (38 GHz) fiber-wireless transmission system using electrical and optical SSB modulation to overcome dispersion effects," *IEEE Photon. Technol. Lett.*, vol. 10, pp. 141–143, Jan. 1998.

[8] L. Y. Lin, M. C. Wu, T. Itoh, T. A. Vang, R. E. Muller, D. L. Sivco, and A. Y. Cho, "High-power high-speed photodetectors-design, analysis, and experimental demonstration," *IEEE Trans. Microwave Theory Tech.*, vol. 45, pp. 1320–1331, Aug. 1997.

[9] M. W. Chbat *et al.*, "Toward wide-scale all-optical transparent networking: The ACTS optical pan-european network (OPEN) project," *IEEE J. Select. Areas Commun., Special Issue on High-Capacity Optical Transport Network*, vol. 16, no. 7, pp. 1226–1244, Sept. 1998.

[10] K. Otsuka, T. Maki, Y. Sampei, Y. Tachikawa, N. Fukushima, and T. Chikama, "A high-performance optical spectrum monitor with high-speed measuring time for WDM optical networks," in *Proc. ECOC'97*, Edinburgh, U.K., Sept. 1997, pp. 147–150.

[11] M. W. Maeda, "Management and control of transparent optical networks," *IEEE J. Select. Areas Commun, Special Issue on High-Capacity Optical Transport Networks*, vol. 16, no. 7, pp. 1008–1023, Sept. 1998.

[12] S. Ohteru and N. Takachio, "Optical signal quality monitor using direct Q-factor measurement," *IEEE Photon. Technol. Lett.*, vol. 11, pp. 1307–1309, Oct. 1999.

[13] F. Heisman *et al.*, "Signal tracking and performance monitoring in multi-wavelength optical networks," in *22nd Eur. Conf. Optical Communication (ECOC '96)*, vol. 3, Oslo, Norway, Sept. 1996, Paper WeB2.2, pp. 47–50.

[14] E. Park *et al.*, "Network demonstration of self-routing wavelength packets using an all-optical wavelength shifter and QPSK subcarrier routing control," in *Conf. Optical Fiber Commun. (OFC '96)*, 1996, pp. 114–115.

[15] R. Gaudino and D. J. Blumenthal, "A novel transmitter architecture for combined baseband data and subcarrier multiplexed control links using differential Mach-Zehnder external modulators," *IEEE Photon. Technol. Lett.*, vol. 19, pp. 1397–1399, Oct. 1997.

[16] R. Gaudino, M. Len, G. Desa, M. Shell, and D. J. Blumenthal, "MOSAIC: A multiwavelength optical subcarrier multiplexed controlled network," *IEEE J. Select. Areas Commun., Special Issue on High-Capacity Optical Transport Networks*, vol. 16, no. 7, pp. 1270–1285, Sept. 1998.

[17] R. Gaudino and D. J. Blumenthal, "WDM channel equalization based on subcarrier signal monitoring," in *Tech. Dig. OFC '98*, San Jose, CA, Feb. 1998, paper WJ6, pp. 167–168.

[18] L. D. Garrett *et al.*, "The MONET New Jersey demonstration," *IEEE J. Select. Areas Commun., Special Issue on High-Capacity Optical Transport Networks*, vol. 16, no. 7, pp. 1199–1219, Sept. 1998.

[19] K. Asahi, M. Yamashita, T. Hosoi, K. Nakaya, and C. Konoshi, "Optical performance monitor built into EDFA repeaters for WDM networks," in *Tech. Dig. OFC'98*, San Jose, CA, Feb. 1998, paper ThO2, pp. 318–319.

[20] R. Wiesmann, O. Bleck, and H. Heppner, "Cost effective performance monitoring in WDM systems," in *Tech. Dig. OFC'2000*, Baltimore, MD, Mar. 2000, paper WK2, pp. 171–173.

[21] S. K. Shin, K. J. Park, and Y. C. Chung, "A novel optical signal-to-noise ratio monitoring technique for WDM networks," in *Tech. Dig. OFC'2000*, Baltimore, MD, March 2000, paper WK6, pp. 182–184.

[22] M. Rasztovits-Wiech, M. Danner, and W. R. Leeb, "Optical signal-to-noise ratio measurement in WDM networks using polarization extinction," in *Proc. ECOC'98*, Madrid, Spain, Sept. 1998, pp. 549–550.

[23] D. K. Jung, C. H. Kim, and Y. C. Chung, "OSNR monitoring technique using polarization-nulling method," in *Tech. Dig. OFC'2000*, Baltimore, MD, Mar. 2000, paper WK4, pp. 176–178.

[24] P. A. Greenhalgh, R. D. Abel, and P. A. Davies, "Optical prefiltering in subcarrier systems," *Electron. Lett.*, vol. 28, no. 19, pp. 1850–1852, Sept. 10, 1992.

[25] G. P. Agrawal, *Fiber-Optic Communication Systems*. New York: Wiley , 1992.

Giammarco Rossi received the "laurea" degree in electronic engineering with honors from the University of Pavia, Italy, in 1994 with a thesis on quantum effects in photodetection. As a Ph.D. student, he worked in the Optoelectronics device research unit of CSELT (Centro Studi E Laboratori Telecomunicazioni, Torino, Italy) and in the Optoelectronic research group of the University of Pavia. He received the Ph.D. degree in electronics in 1999 from the University of Pavia with a dissertation on high-speed semiconductor lasers for advanced optical communication systems.

Dr. Rossi is the recipient of the best thesis in optoelectronics of the year 1999 by the LEOS Italian chapter.

Timothy E. Dimmick received the B.S. degree in electrical engineering from the University of Maryland, College Park, in 1983 and the Ph.D. degree (also from the University of Maryland) in 1990.He is a visitor to the Optical Communications and Photonic Networks (OCPNs) from the Laboratory for Physical Sciences, College Park, MD. His research work includes the development of all fiber narrow-band acoustooptic tunable filters, fiber-optic sensors, optically preamplified receievers, ultrafast diode-pumped solid-state lasers, and coherent light detection and optical signal processing systems. He is currently working to develop optical network performance monitoring techniques using optical subcarrier multiplexed signals.

Daniel J. Blumenthal (S'91–M'93–SM'97) received the B.S.E.E. degree from the University of Rochester, New York, in 1981, the M.S.E.E. degree from Columbia University, New York, in 1988, and the Ph.D. degree from the University of Colorado, Boulder, in 1993.

From 1993 to 1997, he was Assistant Professor in the School of Electrical and Computer Engineering at the Georgia Institute of Technology. He is currently the Associate Director for the Center on Multidisciplinary Optical Switching Technology (MOST) and Associate Professor in the Department of Electrical and Computer Engineering at the University of California, Santa Barbara. He heads the Optical Communications and Photonic Networks (OCPN) Research. His current research areas are in optical communications, wavelength division multiplexing, photonic packet switched and all-optical networks, all-optical wavelength conversion, optical subcarrier multiplexing, and multispectral optical information processing.

Dr. Blumenthal is recipient of a 1999 Presidential Early Career Award for Scientists and Engineers (PECASE) from the White House and the DoD, a 1994 NSF Young Investigator (NYI) Award and a 1997 Office of Naval Research Young Investigator Program (YIP) Award. He is a Member of the Optical Society of America and the Lasers and Electrooptic Society.